ACS OMEGA

http://pubs.acs.org/journal/acsodf

Article

Platelet-Rich Plasma Gel-Loaded Collagen/Chitosan Composite Film Accelerated Rat Sciatic Nerve Injury Repair

Bo Yuan, Xu Zheng, Mo-Li Wu, Yang Yang, Jin-wei Chen, Hui-Chang Gao, and Jia Liu*

Cite This: *ACS Omega* 2023, 8, 2931−2941

Read Online

ACCESS | Metrics & More | Article Recommendations

ABSTRACT: Peripheral nerve injury (PNI) is a common clinical disease caused by severe limb trauma, congenital malformations, and tumor resection, which may lead to significant functional impairment and permanent disability. Nerve conduit as a method for treating peripheral nerve injury shows good application prospects. In this work, the COL/CS composite films with different mass ratios of 1:0, 1:1, and 1:3 were fabricated by combining physical doping. Physicochemical characterization results showed that the COL/CS composite films possessed good swelling properties, ideal mechanical properties, degradability and suitable hydrophilicity, which could meet the requirements of nerve tissue engineering. In vitro cell experiments showed that the loading of platelet-rich plasma (PRP) gel on the surface of COL/CS composite films could significantly improve the biocompatibility of films and promote the proliferation of Schwann cells. In addition, a rat model of sciatic nerve defect was constructed to evaluate the effect of COL/CS composite films on peripheral nerve repair and the results showed that COL/CS composite films loaded with PRP gel could promote nerve regeneration and functional recovery in rats with sciatic nerve injury, indicating that the combination of PRP gel with the COL/CS composite film would be a potential approach for the treatment of peripheral nerve injury.

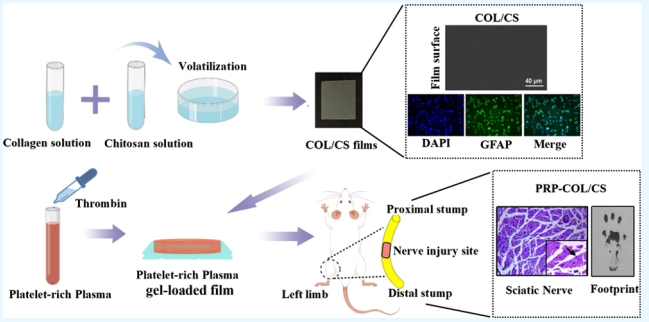

1. INTRODUCTION

Peripheral nerve injury (PNI) is a common clinical disease caused by severe limb trauma, congenital malformations, and tumor resection.[1] It is estimated that about 5 million cases of peripheral nerve injury occur worldwide each year, resulting in severe disability and a reduction in their quality of life.[2−4] At present, the clinical treatment of PNI includes microsurgical suturing of the fractured nerves, autologous nerve grafts, and nonsurgical approaches such as pharmacological, electrical, and laser therapies.[5] Nevertheless, the clinical outcome of these treatments is not optimistic because axon demyelination and degradation often occur in the distal stump of the injured nerve after PNI and result in muscle atrophy and loss of function.[6] It is therefore an urgent need to explore alternative approaches to improve the therapeutic efficacy of PNI.

With the progress of tissue engineering, nerve conduits have been widely used in the treatment of PNI, but they have not yet achieved satisfactory repair outcomes because of invalid regeneration.[7,8] Selection of suitable tissue engineering material to improve nerve regeneration and, meanwhile, to prevent extraneural scarring and adhesion is the main challenge in the field.[9] Type I collagen, as the main component of the extracellular matrix, is widely distributed in mammalian tissues.[10] Due to good biocompatibility, low immunogenicity, and degradability, collagen is regarded as an ideal cell carrier and has been widely used to fabricate biomaterial scaffolds for tissue repair. It has been shown that the transplantation of collagen scaffolds can support chondrocyte repair,[11] cornea repair,[12] and nerve repair.[13] However, collagen has poor biological strength and is subjected to rapid degradation,[14] suggesting the necessity to integrate additional element(s) for generating a composite collagen film with improved physical properties.[15] Chitosan as a kind of natural high polymer polysaccharide may be a potential candidate, which can be gradually degraded to small molecular substances such as glucosamine by the body's lysozyme and possess good antibacterial properties and biocompatibility.[16] It was reported that the composite films composed of collagen and chitosan showed good physical properties and have been applied to wound healing[17] and biomimetic osteochondral tissue construction.[18] Therefore, in this work, we tried to improve the physical properties, mechanical strength, and degradation rate of the collagen film by combining chitosan in the collagen

Received: August 20, 2022
Accepted: December 27, 2022
Published: January 11, 2023

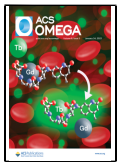

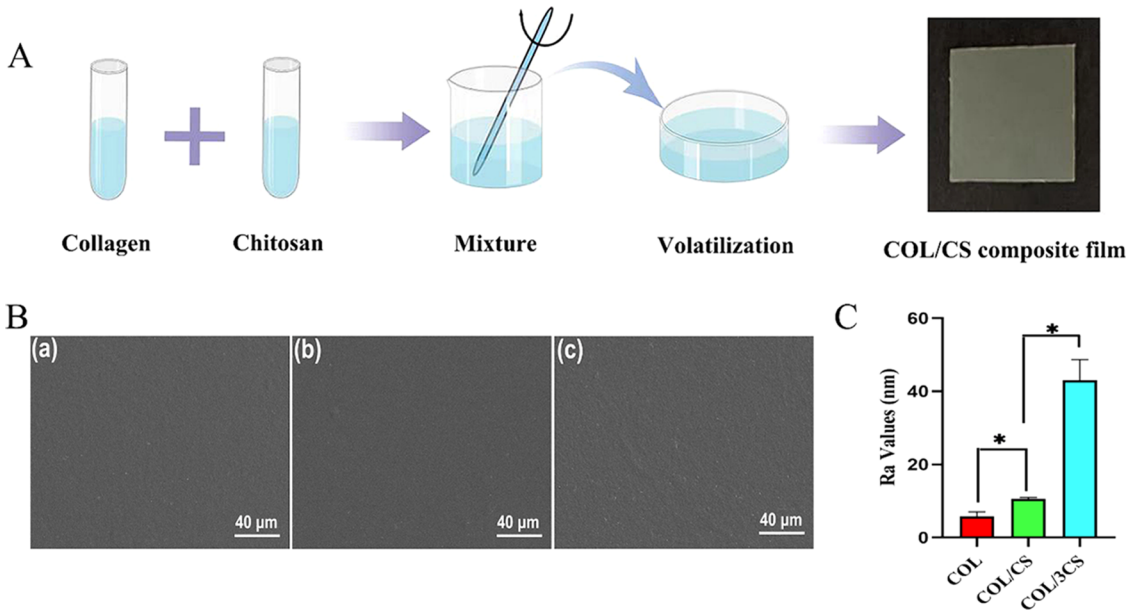

Figure 1. Morphological characterization of COL/CS composite films. (A) Schematic illustration of the COL/CS composite film preparation (drawn with the Figdraw 9 platform). (B) Scanning electron microscopy (SEM) images of the surface of the COL film (a), COL/CS film (b), and COL/3CS film (c). (C) Ra values of different composite films. Values represent the mean ± standard deviation (SD), $n = 5$, $^*p < 0.05$.

film and constructing a nerve catheter for peripheral nerve repair. Nevertheless, the effectiveness of the collagen/chitosan composite film in the management of PNI remains lesser known.

Good biological activity of nerve conduits to promote nerve regeneration is critical for peripheral nerve repair. Platelet-rich plasma (PRP) is an autologous blood-derived concentrate of platelets after the centrifugation of fresh whole blood.[19] Once activated, platelet-rich plasma forms a three-dimensional fibrin gel network containing a variety of growth factors and active proteins including nerve growth factor (NGF), insulin-like growth factor-1 (IGF-1), platelet-derived growth factor (PDGF), and fibroblast growth factor (FGF) that play pivotal roles in nerve healing.[20] The beneficial effects of PRP in the process of injured nerve repair have been evidenced.[21,22] However, the use of PRP is limited due to the rapid elimination from the body when administered via bolus injection. This disadvantage highlights the need for a delivery vehicle for a sustained release of PRP to improve its in vivo therapeutic efficacy. On the other hand, tissue engineering strategies combined with regenerative cells and appropriate delivery vehicles have been proven as one of the most effective approaches to enhance nerve regeneration.[23] It is therefore reasonable to consider that the integration of PRP and collagen/chitosan composite film would be more beneficial in promoting PNI, and this possibility is investigated in the current study using a rat PNI model.

2. MATERIALS AND METHODS

2.1. Materials. Freeze-dried type I collagen (HM Biotech Ltd., Guangzhou, China) was extracted from bovine tendons. The chitosan, 1-(3-dimethylaminopropyl)-3-ethylcarbodiimide hydrochloride (EDC), and *N*-hydroxysuccinimide (NHS) were purchased from Sigma-Aldrich (St. Louis). Lysozyme was supplied by Qiyun Biotechnology Co., Ltd. (Guangzhou, China). Phosphate-buffered saline (PBS, pH = 7.4), Dulbecco's modified Eagle's medium (DMEM), fetal bovine serum (FBS), and other reagents related to cell culture were all purchased from Gibco (Grand Island). Cell counting kit-8 (CCK-8) was purchased from Dojindo Laboratories (Japan). Benzo blue was purchased from Solarbio (Beijing, China). RSC-96 (rat Schwann cells)[24] was purchased from the Cell Bank of the Chinese Academy of Sciences (Shanghai, China).

2.2. Preparation of PRP. The PRP was prepared as previously described.[25] Briefly, 10 mL of whole blood was taken through a heart puncture and loaded into a 15 mL centrifuge tube containing 3.8% w/v of sodium citrate. Then, the whole blood was initially centrifuged at 400*g* for 10 min at 22 °C and separated into three layers. Red blood cells were deposited at the bottom of the tube, and the acellular plasma was located in the upper layer and the platelets, called the buffy coat, were located in the middle layer. Then, the plasma containing platelets was transferred to another sterile tube without an anticoagulant and centrifuged again at 800*g* for 10 min to obtain the platelet concentrate. The upper 2/3 of the platelet-poor plasma was removed, and the lower 1/3 of PRP was suspended by gently shaking the tube. The PRP was activated with 10% calcium chloride (Sigma- Aldrich, St. Louis, Missouri) and a bovine thrombin (Sigma-Aldrich) mixture to obtain the PRP gel (prepared before use). Three hundred microliters of the PRP gel was evenly coated on the surface of the collagen/chitosan composite film to construct the PRP-loaded COL/CS film (the film area was 1.0 cm^2, and the thickness was about 0.1 mm).

2.3. Preparation of COL/CS Composite Films. The COL/CS composite film was prepared by referring to previous reports.[15] Briefly, the type I collagen and the chitosan powders were dissolved in 0.01 mol/L of acetic acid solution. Then, the collagen solution was mixed with the chitosan solution to obtain different mass ratios (COL:CS):COL (1:0), COL/CS (1:1), COL/3CS (1:3). Whereafter, the cross-linking agent EDC and the catalyst NHS were added to the collagen/chitosan solution according to a mass ratio of 6:1:1 (collagen/chitosan:EDC:NHS), and the mixtures were stirred by an electromagnetic stirrer (SP-18, MIULAB, China) for 24 h at a stirring speed of 300 rpm at 4 °C and removing the remaining air in room temperature. Finally, these mixtures were casted into

https://doi.org/10.1021/acsomega.2c05351
ACS Omega 2023, 8, 2931−2941

polystyrene Petri dishes and air-dried to form a composite film (Figure 1A).

2.3.1. Morphology Characterization. To evaluate the effects of different collagen:chitosan composite ratios and PRP loadings on the surface morphology of composite films, the collagen/chitosan composite films with/without PRP-loaded were mounted on an aluminum column and sprayed with a layer of platinum. Then, the surface morphology of films was observed by scanning electron microscope (SEM, EVO18, Zeiss, Germany). In addition, atomic force microscopy (AFM, MFP3D) was also used to scan three different sections (area: 10 μm) of the surface of each film, and the roughness of the sample surfaces was determined.

2.3.2. Mechanical Properties. The collagen/chitosan composite films were first cut into standardized strips (width, 10 mm; length, 30 mm). After equilibrating in PBS, the mechanical properties of the samples were analyzed using a dynamic mechanics analyzer (DMA Q800, TA) at room temperature and a constant speed of 1 N/min. The tensile strength and elongation rate of the wet composite films were determined. Every reported value was the average of at least five measurements. The elastic modulus under extension was calculated as the slope of the linear portion of the stress−strain curve between 10 and 20% strain.

2.3.3. Water Content Measurement. The equilibrated water content of the composite films was determined by referring to the previous method.[15] In brief, the dry collagen/chitosan composite films were weighed W_0 and then immersed in PBS. At regular time intervals, the wet weight of the composite films (W_t) was measured after gently blotting the surface water with filter paper. The water contents of the films were calculated using the following equation

$$\text{water absorption} = (W_t - W_0)/W_t \times 100\%$$

2.3.4. In Vitro Degradation. To evaluate the effects of different collagen:chitosan composite ratios on the degradation rate of composite films, in vitro degradation test was performed. In brief, after being weighed, the composite films fully equilibrated with water were placed in 5 mL of PBS, which contains lysozyme (5 U/mL). Then, the composite films were incubated at 37 °C and their weight was recorded at different times until the composite films were degraded completely. The residual mass of films was normalized according to the following formula, where W_t is the weight of films at a specific time and W_0 is the initial weight of films. Every reported value was the average of a least five measurements

$$\text{relative residual mass} = W_t/W_0 \times 100\%$$

2.3.5. Contact Angle Measurement. To evaluate the effects of different collagen:chitosan composite ratios on the hydrophilicity of composite films, after being saturated in saline solution, the contact angle of ultramorphic water on the surface of composite films was measured at room temperature (25 °C). The droplet volume was 2 μL, and the droplet velocity was medium. Five points were randomly selected for each sample.

2.3.6. Cytotoxic Evaluation. CCK-8 assay was used to determine the effects of COL/CS films on the metabolic activity of RSC-96 cell at different time intervals. In brief, RSC-96 cells were seeded on the COL film, COL/CS film, COL/3CS film, and PRP-loaded COL/CS film at a density of 1×10^4 cells/well. After culturing for 24 and 48 h, the CCK-8 working solution was added and incubated at 37 °C for 2.5 h. Subsequently, the supernatant medium was extracted for absorbance detection by a Thermo 3001 microplate reader (Thermo) ($n = 5$) at 450 nm. In addition, trypan blue exclusion assay was also performed to evaluate the viability of cells. Cells were treated with trypan blue dye (0.2%) and counted with a hemocytometer. Furthermore, DAPI/GFAP fluorescence double staining was used to observe cell morphology by immunofluorescence microscope. Briefly, RSC-96 cells were incubated on the plate, COL film, COL/CS film, COL/3CS film, and PRP-loaded COL/CS film for 24 h. Then, cells were fixed with 4% paraformaldehyde for 20 min and blocked in PBS supplemented with 5% bovine serum albumin for 30 min. Subsequently, polyclonal anti-GFAP antibody (1:300, Cat no: 16825-1-AP, Proteintech) was added and incubated overnight at 4 °C. After rinsing with PBS two times (5 min per wash), Alexa Fluor 594-conjugated antirabbit IgG (1:500, Invitrogen) and 5 μg/mL of DAPI (Beyotime, China) in incubation buffer were added and incubated for 1 h at room temperature. After rinsing with PBS two times (5 min per wash), cell morphology was observed and photographed using a fluorescence microscope (Leica, DMI4000B, Germany).

2.4. In Vivo Studies. *2.4.1. Rat Peripheral Nerve Injury Model and Treatments.* The contents of animal experiments and animal care were strictly carried out according to Chinese Animal Welfare Guidelines and approved by the Ethical Committee for Animal Experiments of Dalian Medical University (no. AE18055, Dalian, China). Twenty-five male SD rats (10 weeks old, 300 ± 10 g, provided by the Laboratory Animal Center, Dalian Medical University) used in the animal experiments were randomly divided into five groups (five rats/group): untreated control (UC; with injury but without interventions); sham-operated as a positive control (SC); nerve suture (NS; the sciatic nerve was severed and microstitched with 8-0 lines); collagen/chitosan (COL/CS; surrounds the nerve anastomotic end with the collagen/chitosan composite film after the sciatic nerve suture); collagen/chitosan/platelet-rich plasma (PRP-COL/CS; surrounds the nerve anastomotic end with the PRP gel-carrying collagen/chitosan composite film after the sciatic nerve suture). For the surgical procedure, the animals were anesthetized with 1% pentobarbital sodium (40 mg/kg), and a skin incision was made at the left lower limb of the rats.[26] The sciatic nerve at 1.5 cm exiting from the pelvis was exposed and cut using ophthalmic scissors, and the nerve was microstitched with 8-0 lines. The COL/CS film and PRP gel-loaded COL/CS film were used to wrap the nerve anastomosis. The incision was closed using 3-0 silk sutures.

2.4.2. Walking-Footprint Analysis. The rat footprints were recorded at 4 and 8 weeks postoperatively and subjected to sciatic nerve function index analysis. In brief, the rats' hind paws were first soaked in the ink. Then, the rats were placed inside an acrylic corridor (100 cm length, 7 cm width, and 6 cm height) lined with a millimeter paper and ended with a darkened goal box. The sciatic functional index (SFI) was calculated by the following formula, where the print length (PL) represents the distance from the heel to the top of the third toe; intermediate toe spaces (IT) represent the first and third toe spacing; and toe spread (TS) represents the second and fourth toe spacing. NPL, NTS, and NIT represent the PL, IT, and TS values of the nonsurgical side hind limb, respectively. EPL, ETS, and EIT represent the PL, IT, and TS values on the surgical side of the experimental animals, respectively. The closer the SFI value is to 0, the better the function recovery. An SFI value of 100 represents a complete loss of function. The sciatic functional index values for five rats in each group were averaged.[27]

https://doi.org/10.1021/acsomega.2c05351
ACS Omega 2023, 8, 2931−2941

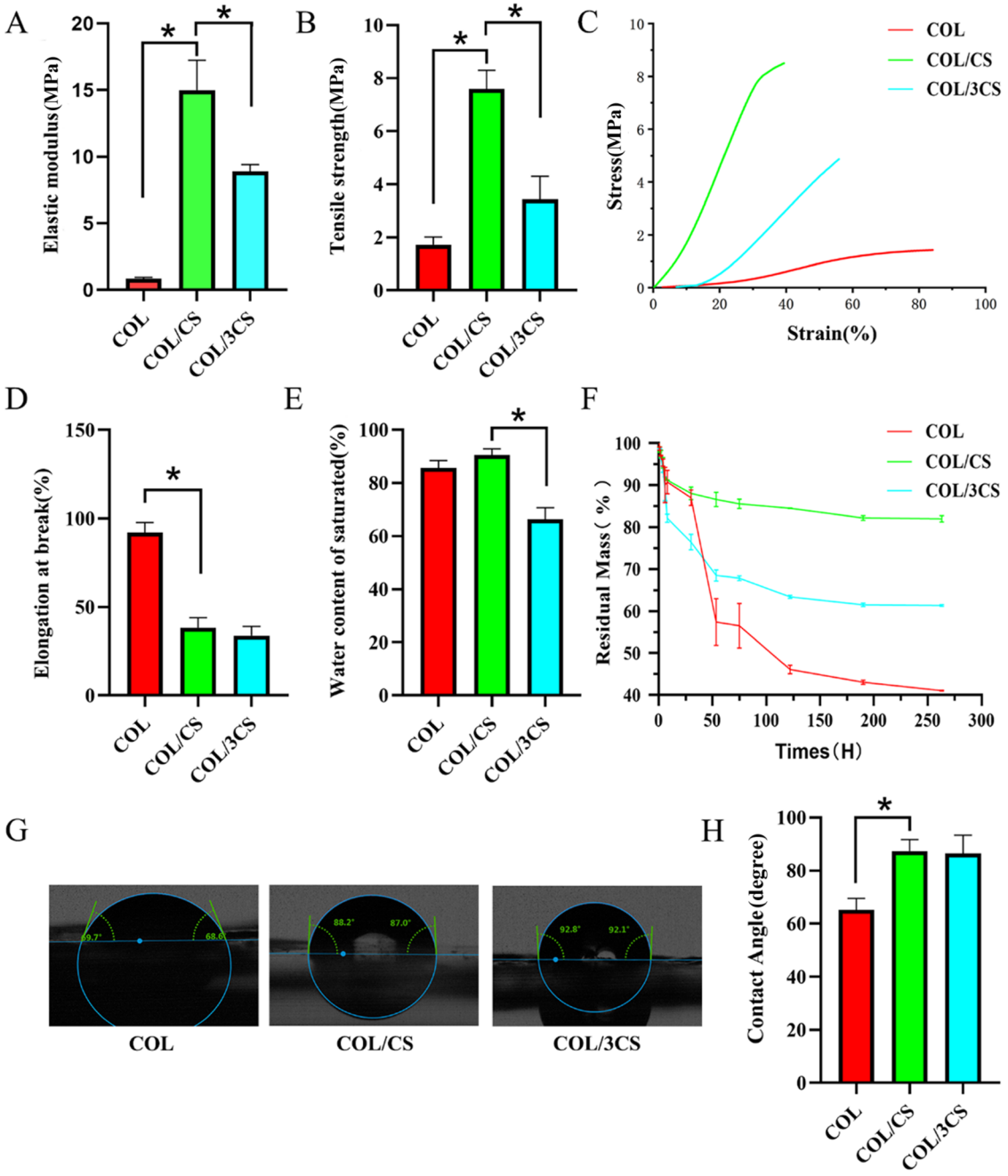

Figure 2. Physicochemical properties of COL/CS composite films. Histogram comparing the tensile mechanical properties of the COL film, COL/CS film, and COL/3CS film, including (A) elastic modulus, (B) tensile strength, (C) stress−strain curves, and (D) elongation at break. (E) Histogram comparing the water content of COL/CS composite films. (F) The lysozyme-mediated biodegradation of the COL/CS composite films after absorbing water at different times. (G) Images of the water contact angle of films. (H) Quantitative comparative analysis of contact angles of COL/CS composite films. Values represent the mean ± SD, $n = 5$, $^*p < 0.05$.

$$\mathrm{SFI} = \frac{-38.3 \times (\mathrm{EPL} - \mathrm{NPL})}{\mathrm{NPL}} + \frac{109.5 \times (\mathrm{ETS} - \mathrm{NTS})}{\mathrm{NTS}} + \frac{13.3 \times (\mathrm{EIT} - \mathrm{NIT})}{\mathrm{NIT}} - 8.8$$

2.4.3. Hot Plate Latency Test. Hot plate test was performed 8 weeks after surgery by placing the injured limb of rats on a hot plate at 56 °C.[28] The reaction time was considered the interval between the moment the animal was placed on the plate and the time it started licking its claws or raising its hands.[29] The cut of time point was considered 12 s, and the animals that showed no reaction at this time point were excluded from the study. The reaction time for five rats in each group was averaged.

2.4.4. Gastrocnemius Muscle Wet Weight Loss. At the end of 8 weeks post surgery, the animals were euthanized by CO_2, and the posterior gastrocnemius muscles on the injured and uninjured hind limbs were harvested and immediately weighed to determine the wet weight loss of muscles using the following equation.[30]

https://doi.org/10.1021/acsomega.2c05351
ACS Omega 2023, 8, 2931−2941

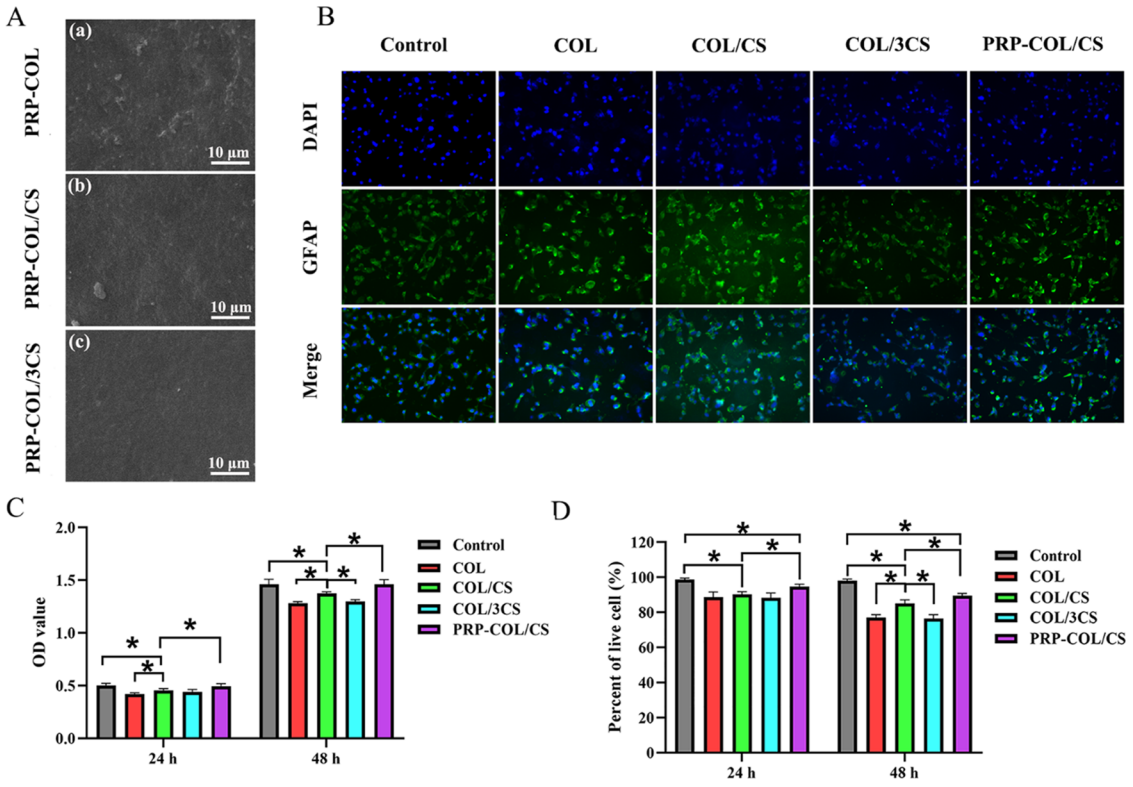

Figure 3. Biocompatibility evaluation of COL/CS composite films loaded with PRP gel. (A) SEM images of the surface of (a) PRP-loaded COL film, (b) PRP-loaded COL/CS film, and (c) PRP-loaded COL/3CS film. (B) DAPI/GFAP fluorescence double staining images of cell metabolism of RSC-96 cells cultured on the plate, COL film, COL/CS film, COL/3CS film, and PRP-loaded COL/CS film for 24 h. (C) Histogram comparing the proliferation of RSC-96 cells cultured for 24 and 48 h using CCK-8 assay and (D) trypan blue exclusion assays. Values represent the mean ± SD, $n = 5$, $^*p < 0.05$.

$$\text{gastrocnemius muscle wet weight} - \text{loss} = \left(1 - \frac{\text{wet weight of muscle on the injured side}}{\text{wet weight of muscle on the uninjured side}}\right) \times 100$$

2.4.5. Histopathological and Immunohistochemical Examinations. Tissues from the gastrocnemius muscle and sciatic nerve were collected and fixed with 10% formalin, dehydrated with graded ethanol, and embedded with paraffin to prepare 5 μm thick continuous slices. Hematoxylin and eosin (H&E) staining, including hematoxylin staining for 2.5 min, eosin staining for 3 min, 1% hydrochloric acid differentiation, ethanol gradient dehydration, and neutral gum seal, was performed according to the routine procedure at 20−23 °C prior to the light microscope (Leica Microsystems, Germany) observation of histopathological changes. In addition, immunohistochemical (IHC) staining was also performed as previously described.[31] Briefly, 5 μm paraffin-embedded sciatic nerve tissue sections were deparaffinized in xylene and then rehydrated in a serial gradient of ethanol and washed with PBS. Tissue sections were further quenched sequentially by using 3% hydrogen peroxide for 15 min and incubated in 10% normal goat serum (ZSGB-BIO, Beijing, China) for 45 min at room temperature. The slides were then incubated at 4 °C overnight with monoclonal anti-S-100β (1:200, Cat no: 66616-1-Ig, Proteintech) or polyclonal anti-GFAP antibody (1:200, Cat no: 16825-1-AP, Proteintech). After rinsing with PBS, the slides were incubated with a horseradish peroxidase-conjugated goat antirabbit IgG for 30 min at 37 °C. 3-Diaminobenzidine tetrahydrochloride (DAB) (ZSGB-BIO, Beijing, China) was used as the chromogen, and hematoxylin (KeyGEN-Bio, China) was used for nuclear counterstaining. For negative controls, the primary antibodies were omitted. The IHC photos were taken using a light microscope (Leica Microsystems, Germany). Image analysis was conducted using ImageJ (National Institutes of Health).

2.4.6. Statistical Analysis. All data were expressed as mean ± standard deviation (SD). One-way analysis of variance (ANOVA) was conducted using SPSS 22.0 software (IBM Corp.). A value of $P < 0.05$ was considered to indicate a statistically significant difference.

3. RESULTS

3.1. Morphological Characterization of COL/CS Composite Films. The COL/CS composite films with collagen:-chitosan mass ratios of 1:0, 1:1, and 1:3 (COL, COL/CS, and COL/3CS) were fabricated by combining physical doping (Figure 1A). To evaluate the effect of chitosan incorporation on the collagen composite film, the surface morphology of composite films was observed by SEM and the results are shown in Figure 1B. The surface of the composite films was smooth and flat, and the combination of collagen and chitosan was also uniform, indicating that the COL/CS composite films were successfully prepared. However, it was found that the surface of the composite films became more roughened with the increase of the content of chitosan compared with the collagen film. Furthermore, the surface roughness of composite films was checked by AFM. As shown in Figure 1C, the roughness of the COL/CS composite films became increased ($P < 0.05$) in a

https://doi.org/10.1021/acsomega.2c05351
ACS Omega 2023, 8, 2931−2941

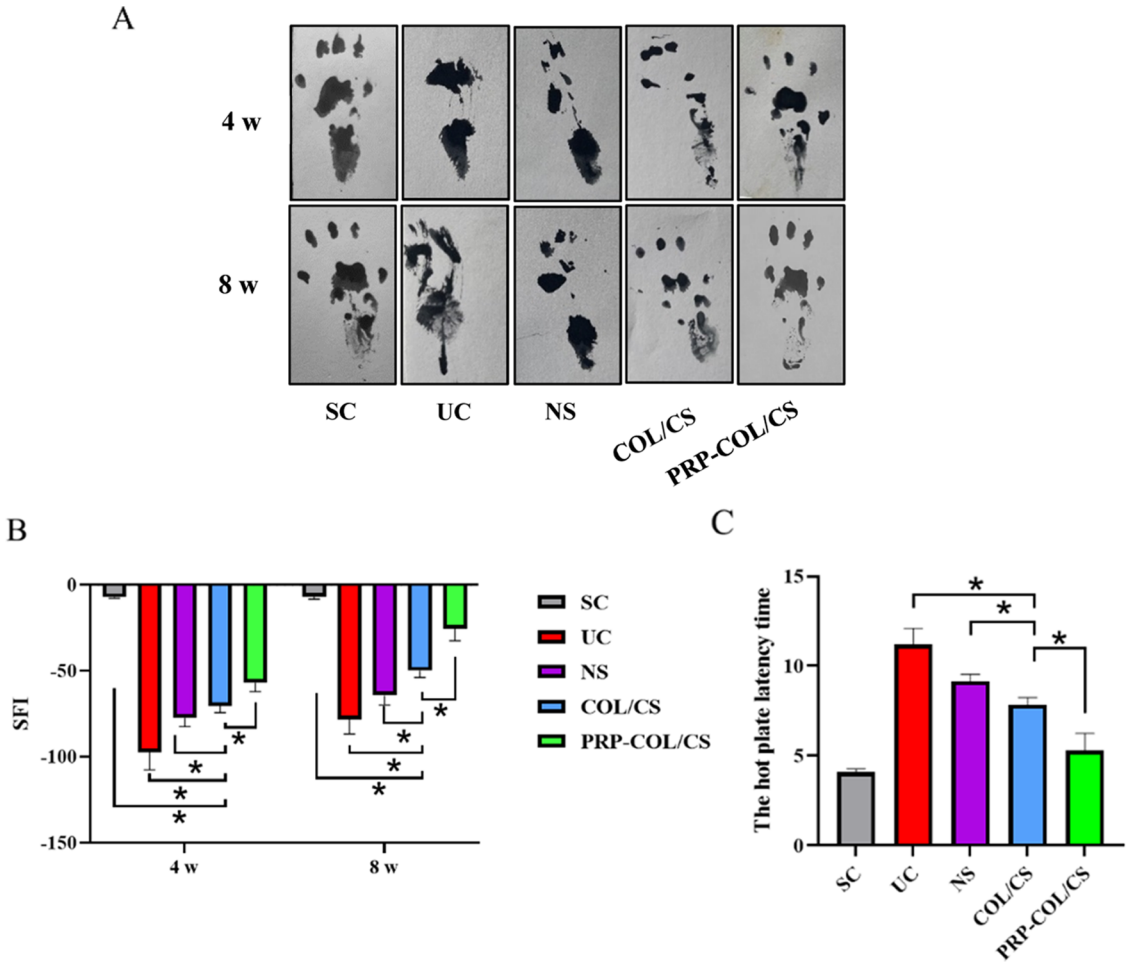

Figure 4. COL/CS composite film facilitates neurologic functional recovery after SNI. (A) Representative images of the footprint of different groups. (B) Histogram comparing the sciatic functional index (SFI) at 4 and 8 weeks after surgery. (C) Histogram comparing the hot plate latency time at 8 weeks after surgery. Values represent the mean ± SD, $n = 5$, $^*p < 0.05$.

chitosan dose-related fashion, consistent with the results of SEM.

3.2. Physicochemical Properties of COL/CS Composite Films. The effects of different contents of chitosan on the physicochemical properties of collagen-based materials were evaluated, including mechanical properties, saturated water content, in vitro degradation, and surface hydrophilicity. The results of the mechanical strength test are shown in Figure 2A–D and found that the introduction of chitosan could improve the mechanical properties of collagen-based materials. When the mass ratio of collagen and chitosan is 1:1, the composite films had the best elastic modulus (15.00 ± 2.3 MPa) and tensile strength (7.59 ± 0.70 MPa), indicating that the optimum composite ratio of collagen and chitosan could form the best composite structure. Moreover, the COL/CS film group has a lower elongation at break (38.3 ± 5.6%) compared with the COL film (Figure 2D). In addition, there was no significant difference in the saturated water content between the COL/CS film and COL film, while the saturated water content was higher than the COL/3CS composite film ($P < 0.05$) (Figure 2E). These results indicated that the COL/CS film had a similar water content to the COL film when the composite ratio of collagen and chitosan was 1:1. In vitro degradation results showed that the COL/CS film had the slowest degradation rate of all of the groups, followed by the COL/3CS film, and COL film had the fastest degradation rate (Figure 2F). The effect of chitosan composite on the surface hydrophilicity of the films was studied, and the results are shown in Figure 2G,H. Although the addition of chitosan could decrease the surface hydrophilicity of the composite films compared with that of the pure collagen film, the contact angle of the COL/CS film and the COL/3CS film is about 90°, which was suitable for cell adhesion and growth. The above results indicated that the introduction of chitosan could effectively improve the physicochemical properties of collagen membrane, among which the COL/CS film has the best performance and was suitable for the construction of nerve conduits.

3.3. Biocompatibility Evaluation of COL/CS Composite Films Loaded with PRP Gel. The surface morphology of COL/CS composite films loaded with PRP gel was first observed by SEM, and the results are shown in Figure 3A. It was found that the PRP gel could be well bonded on the surface of COL/CS composite films and the surface became rough. To investigate the effect of COL/CS composite films on the proliferation and viability of RSC-96 cells, especially after loading PRP gel, DAPI/GFAP double staining, CCK-8, and trypan blue exclusion assays were performed to access cell growth and viability. Immunofluorescence staining for GFAP was used to label Schwann cells, whereas DAPI was used to label cell nuclei. The results revealed that more staining cells were found in the control groups and PRP-COL/CS groups than in the COL and COL/3CS groups (Figure 3B). The cell numbers

https://doi.org/10.1021/acsomega.2c05351
ACS Omega 2023, 8, 2931−2941

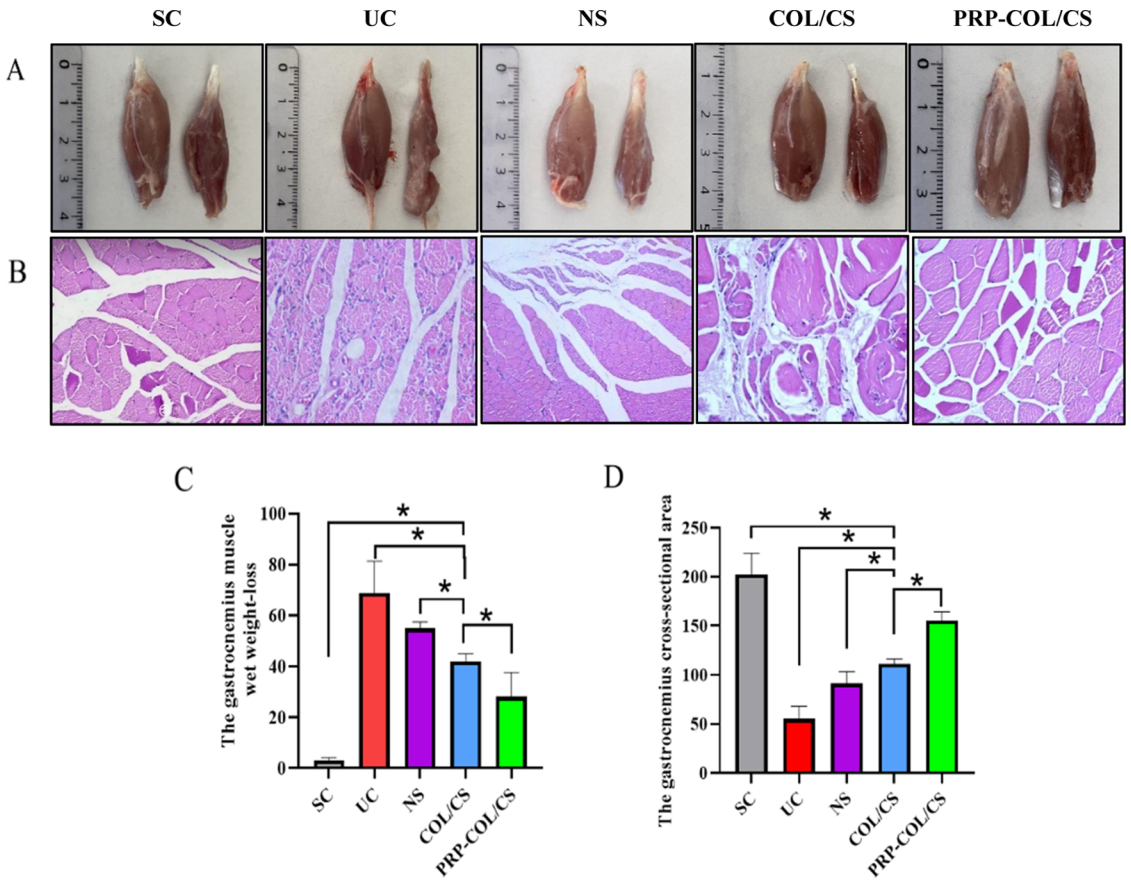

Figure 5. COL/CS composite film attenuated muscle atrophy after SNI. (A) Representative pictures of normal limb muscle (left) and affected limb muscle (right). (B) Micrographs of gastrocnemius muscle stained by hematoxylin and eosin (H&E) at 8 weeks after surgery (×200 magnification). (C) Histogram comparing the gastrocnemius muscle wet weight loss at 8 weeks after surgery. (D) Histogram comparing the cross-sectional area of the gastrocnemius muscle at 8 weeks after surgery. Values represent the mean ± SD, $n = 5$, $^*p < 0.05$.

cultured on COL/CS films were reduced to an extent of 9.43%, 8.34% and 5.9%, 5.82% at 24 and 48 h, respectively, in comparison with that of the control group and PRP-COL/CS group, and increased to 7.41%, 6.09% than the COL group and COL/3CS group at 48 h (Figure 3C). In addition, the results of trypan blue staining showed that the cell viability was more than 80% and the cell viability rates of COL/CS-treated were reduced to an extent of 8.39%, 4.62% and 13.3%, 5.0% at 24 and 48 h, respectively, in comparison with that of the control group and PRP-COL/CS group, and were higher by 10.44%, 11.10% than the COL group and COL/3CS group at 48 h (Figure 3D). These results demonstrated that the loading of PRP gel on the surface of COL/CS composite films could significantly improve the biocompatibility of films and promote the proliferation of nerve cells.

3.4. COL/CS Composite Film Facilitated Neurologic Functional Recovery. The nerve regeneration efficacy of the COL/CS composite films was evaluated in the sciatic nerve defect animal model, and the healing process was assessed via anatomical and functional evaluations. As shown in Figure 4A,B, the implantation of COL/CS composite films significantly improved SFI at both 4 and 8 weeks post surgery compared with that of NS and UC groups. SFI values of the PRP-COL/CS group at 4 and 8 weeks post surgery were −57.02 ± 5.15 and −25.57 ± 7.03, respectively, which were significantly higher than those of the COL/CS group. In addition, the hot plate latency test was also carried out to evaluate the recovery of thermal pain sensitivity on the injured limb of rats, and the results are presented in Figure 4C. The latency for the COL/CS group was 7.84 ± 0.40 s, which was lower than NS and UC groups. The value of the RP-COL/CS group was 5.28 ± 0.97 s, which was significantly lower than that of the COL/CS groups.

3.5. COL/CS Composite Film Attenuated Post-SNI Muscle Atrophy. In this study, the regenerative effect of sciatic nerve injury was indirectly assessed by using H&E staining and the gastrocnemius weight loss. As shown in Figure 5A, the affected limb muscle was smaller than the normal limb in the UC group, while there were few differences between the affected limb muscle and normal limb muscle in the PRP-COL/CS group. The muscular cells were atrophied and disorganized in the UC group, whose severity was higher than that of the COL/CS group. The PRP-COL/CS group provided muscle fibers similar to the SC group with a typical structure and well-defined cell border, while myocyte atrophy was still present (Figure 5B). Moreover, the COL/CS group had a gastrocnemius muscle wet weight loss with 42.0 ± 3.0% at 8 weeks after surgery, which was significantly lower than NS and UC groups. The percentage in the PRP-COL/CS group was 28.0 ± 9.7%, which was significantly lower than that in the COL/CS groups (Figure 5C). The gastrocnemius muscle cross-sectional area was progressively increased in the PRP-COL/CS group compared with that in the UC, NS, and COL/CS groups (Figure 5D).

3.6. COL/CS Composite Film Improved Nerve Morphology after SNI. The nerve repair effect of the COL/CS film was also assessed by the morphological observation of H&E and

https://doi.org/10.1021/acsomega.2c05351
ACS Omega 2023, 8, 2931−2941

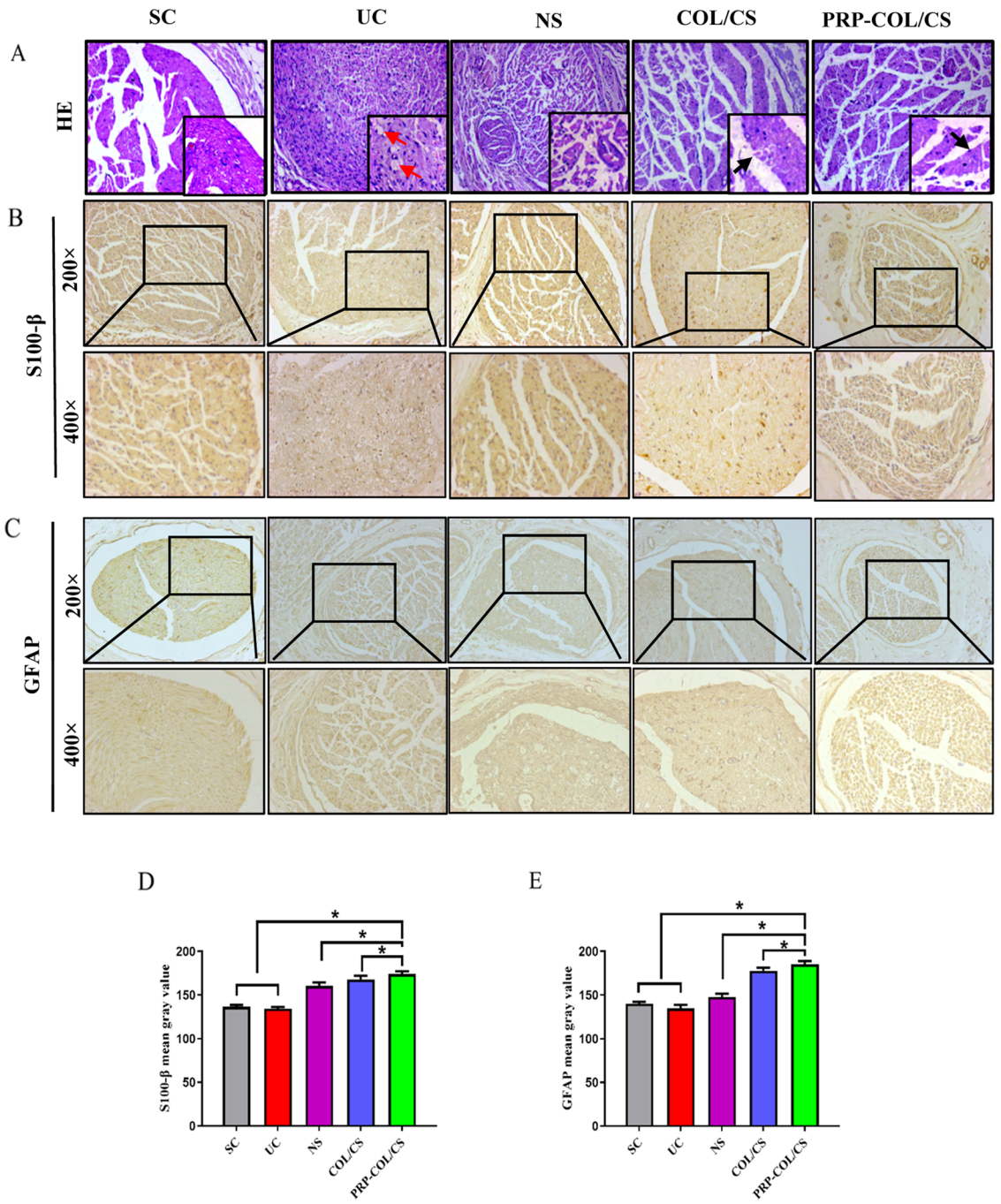

Figure 6. COL/CS composite film improved nerve morphology following SNI in rats. (A) Micrographs of the sciatic nerve stained by hematoxylin and eosin (H&E) at 8 weeks after nerve injury (×200 magnification and bottom right is ×400 magnification). The red arrow indicates nerve fiber vacuolation; the black arrow indicates myelin sheath. Immunohistochemical analysis of (B) S-100β and (C) GFAP. (D) Quantitative analysis of the S-100β mean gray value. (E) Quantitative analysis of the GFAP mean gray value. Values represent the mean ± SD, n = 5, *p < 0.05.

immunohistochemical-stained nerve repair tissues. As shown in Figure 6A, the UC group had disordered nerve fibers and swollen or missing axons, indicating varying degrees of edema and vacuolization. Histopathological evaluation of the NS group also showed different degrees of edema and vacuolization of myelin and mild edema around the nerve fibers. There was a significant improvement in both myelin regeneration and fiber status in the COL/CS group. The symptoms of nerve injury were reduced, and only mild vacuolization was seen. In the PRP-COL/CS group, there was a significant improvement in remyelination and fiber status, and the intact myelin sheaths and well-arranged fibers were more similar to normal sciatic nerves. In addition, the immunohistochemical examination of S-100β and GFAP proteins was carried out in cross sections of regenerated nerve segments. As shown in Figure 6B–E, the results showed that the PRP-COL/CS group had the highest gray value, which was higher by 3.55%, 3.99% than the COL/CS group, which demonstrated increased nerve repair. Besides, the gray value of S-100β and GFAP in the COL/CS groups were higher by 19.96%, 24.22% than that in the UC group.

https://doi.org/10.1021/acsomega.2c05351
ACS Omega 2023, 8, 2931−2941

4. DISCUSSION

Peripheral nerve injury (PNI) is a devastating condition that may result in the loss of sensory function and motor function. PNI can be caused by different damaging factors and therefore have a high worldwide incidence.[32] Despite the technical progression of microsurgery, the therapeutic outcome of PNI is still unfavorable due to the extremely weak regenerative capacity of the injured neurons and the presence of Schwann cells within the denervated nerve stumps.[33] Apparently, the promotion of neuronal regeneration and, meanwhile, the prevention of other cell invasions to the stump regions are critical to accelerating wounded nerve healing and are therefore of clinical significance. To reach that goal, it is necessary to use some degradable biomaterials such as collagen[34] and chitosan[35] as the major components of tissue engineering scaffold.

It has been found that tissue engineering materials containing collagen and/or chitosan can effectively improve wound repair quality.[36] Collagen I as the essential component of the ECM shows good biocompatibility and is involved in cell adhesion, proliferation, migration, and differentiation,[37,38] but, on the other hand, collagen has poor mechanical strength and its physical properties need to be improved by adding other compounds to generate composite collagen films with mechanical strength and interaction between the collagen molecular chains.[39] Moreover, the additional composite material should be nontoxic and easy to prepare. Chitosan is such a candidate because of its good biocompatibility, biodegradability, and mechanical strength as well as cellular safety.[17,18,40] For these reasons, the COL/CS composite films in different formulas were constructed for investigating their influence on PNI repair and regeneration. In this study, the comparison of the biophysical properties of pure collagen films and COL/CS composite films with different COL:CS ratios showed that the composite film with a mass ratio of 1:1 COL to CS demonstrated the best swelling property, tensile strength, and longest degradation time in vitro. These results indicated that the COL/CS film was not prone to deformation when subjected to a certain external force. This film was also conducive to nutrient exchange because of its ideal hydrophilicity.[41] The above results suggested that the COL/CS film, as a biological scaffold, would be more suitable for investigations.

As a tissue engineering study, the interactions between nerve cells and scaffold materials are our main focus, because this is the basis for the growth of regenerative axons through the site of injury.[42] Cell migration, differentiation, and proliferation require proper adhesion between cells and materials.[43] In this study, the COL/CS composite film loaded with PRP gel was characterized by SEM, and it was found that the PRP gel uniformly adhered to the surface of the composite film. The CCK-8 labeling, trypan blue exclusion assay, and DAPI/GFAP fluorescence double staining were performed and proved that RSC-96 cells cultured on the COL/CS film possessed good cytocompatibility in vitro. RSC-96 is a rat-derived Schwann cell line, which kept on growing in the COL/CS film-treated group although its proliferation was slightly lower (20%) than that of normally cultured ones. This finding was consistent with the results reported by Chu et al.[44] However, the cell metabolic activity was significantly higher after the COL/CS film was loaded with PRP, indicating that PRP could promote the growth of RSC-96 cells on the COL/CS film, which also illustrated that additional bioactive factors are necessarily integrated or loaded onto it to improve the therapeutic outcome.[44,45]

Platelet-rich plasma (PRP) is an autologous blood-derived product with high amounts of platelets and concentrated growth factors within a small volume of plasma.[46] Therefore, PRP has been used as a safe and novel preparation for clinical peripheral neuropathies.[47] Nevertheless, the use of PRP is limited due to the rapid elimination from the body when administered via bolus injection.[48] This disadvantage highlights the need for a delivery vehicle for a sustained release of PRP to improve its in vivo therapeutic efficacy. In this context, chitosan would be suitable carriers by which the PRP gel can slowly release the growth factors from PRP-loaded chitosan scaffolds and elongate its biological effects. By this way, the lack of growth factors in the COL/CS film and the difficulty to maintain long-term in vivo effects of the PRP gel are largely overcome. In this study, we prepared PRP gel from rat whole blood by the method used elsewhere[25] and then loaded it onto the prepared COL/CS film. We then elucidated the efficacy of the COL/CS film with a 1:1 mass ratio-loaded PRP for rat sciatic nerve damage repair. The SFI is a widely used indicator to evaluate the recovery of peripheral nerve function. After sciatic nerve injury, limb coordination decreases, affecting fine movements of the hind limb, and thus SFI values decrease. Our results showed that the SFI value of the PRP-COL/CS group was significantly increased compared with that of COL/CS and NS groups, indicating that the PRP gel-COL/CS composite film could promote the recovery of hind limb motor function in rats with sciatic nerve injury. Hot plate latency experiment showed that rats in the PRP-COL/CS group were more sensitive to pain temperature perception. Muscle atrophy is a common complication of PNI, which can be improved through nerve regeneration and functional recovery. Our results showed that the recovery of muscle atrophy and morphology in the PRP-COL/CS group was more obvious than that in the other groups, indicating the efficacy of the PRP gel-loaded COL/CS composite film in promoting nerve regeneration, functional reconstruction, and muscle recovery. In addition, the physicochemical analyses demonstrated that the PRP gel-loaded COL/CS composite film could improve SFI and reduce the thermal plate latency of the film. The PNI rats treated with the PRP-COL/CS film showed increased gastrocnemius muscle weight rate, improved nerve tissue morphology, and accelerated nerve regeneration and functional recovery. These findings thus suggested the potential value of this combination formula in the better management of PNI.

Schwann cells have good plasticity in the repair process and can develop into myelin-forming Schwann cells (MSCs) and nonmyelinated Schwann cells (NMSCs), which are the core of the regenerative potential of the peripheral nervous system.[49] The phenotypic changes of Schwann cells indicate the state of Schwann cells and the extent of PNI lesions. S-100β and GFAP are specific marker proteins of Schwann cells. S-100β is mainly expressed in MSCs and GFAP in NMSCs in peripheral nerves. The S-100β protein family is an acidic calcium-binding protein that can serve as a marker of functional activation after nerve injury. Nerve injury may trigger in vivo repair systems, including the activation of S-100β protein overexpression and promotion of nerve regeneration.[50] GFAP is predominantly expressed in astrocytes of the CNS tissue. In the periphery, GFAP is only found when regeneration or other dynamic processes occur after nerve damage.[51] It is reported that after sciatic nerve transection, axonal degeneration stimulated MSCs to acquire a phenotype similar to that of NMSCs with increased GFAP expression, morphological changes, and neurite extension.[52] In the UC

https://doi.org/10.1021/acsomega.2c05351
ACS Omega 2023, 8, 2931−2941

group, nerve fibers were disorderly arranged, swollen, and undergone varying degrees of edema and vacuolization. This situation could be improved in the COL/CS group and especially in the PRP-COL/CS group. In addition, both S-100β protein and GFAP expression levels increased significantly after the PRP-COL/CS film treatment, indicating that this film could promote Schwann cell proliferation, nerve regeneration, and, finally, functional recovery.

5. CONCLUSIONS

The COL/CS composite films with different mass ratios of 1:0, 1:1, and 1:3 were successfully fabricated by combining physical doping in this study. Physicochemical characterization results showed that the COL/CS composite films possessed good swelling properties, ideal mechanical properties, degradability, suitable hydrophilicity and good cell compatibility, which could meet the requirements of neural tissue engineering. In addition, a rat model of sciatic nerve defect was constructed to evaluate the effect of COL/CS composite films on peripheral nerve repair and the results showed that COL/CS composite films could promote nerve regeneration and functional recovery in rats with sciatic nerve injury, especially when the PRP gel was loaded on it. Overall, our experimental results demonstrated that a combination of PRP gel with the COL/CS composite film would be a potential approach for the better treatment of peripheral nerve injury.

AUTHOR INFORMATION

Corresponding Author

Jia Liu − *Liaoning Laboratory of Cancer Genomics and Epigenomics, College of Basic Medical Sciences, Dalian Medical University, Dalian 116044, China; South China University of Technology School of Medicine, Guangzhou 510006, China*; Email: jialiudl@dmu.edu.cn, mcliujia@scut.edu.cn

Authors

Bo Yuan − *Liaoning Laboratory of Cancer Genomics and Epigenomics, College of Basic Medical Sciences, Dalian Medical University, Dalian 116044, China*; orcid.org/0000-0002-7503-1499

Xu Zheng − *Liaoning Laboratory of Cancer Genomics and Epigenomics, College of Basic Medical Sciences, Dalian Medical University, Dalian 116044, China*

Mo-Li Wu − *Liaoning Laboratory of Cancer Genomics and Epigenomics, College of Basic Medical Sciences, Dalian Medical University, Dalian 116044, China*

Yang Yang − *Liaoning Laboratory of Cancer Genomics and Epigenomics, College of Basic Medical Sciences, Dalian Medical University, Dalian 116044, China*

Jin-wei Chen − *South China University of Technology School of Medicine, Guangzhou 510006, China*

Hui-Chang Gao − *South China University of Technology School of Medicine, Guangzhou 510006, China*; orcid.org/0000-0001-8860-2118

Complete contact information is available at: https://pubs.acs.org/10.1021/acsomega.2c05351

Notes

The authors declare no competing financial interest.

ACKNOWLEDGMENTS

This work was supported by grants from the National Natural Science Foundation of China (Nos. 81272786, 81450016), the Basic Scientific Research Fund for Natural Science Subjects from the South China University of Technology, Guangdong Provincial Science and Technology Innovation Strategy Fund (Cultivation of college students' scientific and technological innovation) (Grant No.: pdjh2021b0039), and the cultivating scientific research project of the Second Hospital of Dalian Medical University (Grant No.: dy2yynpy202219).

REFERENCES

(1) Modrak, M.; Talukder, M.; Gurgenashvili, K.; Noble, M.; Elfar, J. C. Peripheral Nerve Injury and Myelination: Potential Therapeutic Strategies. *J. Neurosci. Res.* **2020**, *98*, 780−795.

(2) Hopf, A.; Schaefer, D. J.; Kalbermatten, D. F.; Guzman, R.; Madduri, S. Schwann Cell-Like Cells: Origin and Usability for Repair and Regeneration of the Peripheral and Central Nervous System. *Cells* **2020**, *9*, No. 1990.

(3) Qin, J.; Wu, J. C.; Wang, Q. H.; Zhou, S. L.; Mao, S. S.; Yao, C. Transcription Factor Networks Involved in Cell Death in The Dorsal Root Ganglia Following Peripheral Nerve Injury. *Neural Regener. Res.* **2018**, *13*, 1622−1627.

(4) Scaccini, L.; Mezzena, R.; De Masi, A.; Gagliardi, M.; Gambarotta, G.; Cecchini, M.; Tonazzini, I. Chitosan Micro-Grooved Membranes with Increased Asymmetry for the Improvement of the Schwann Cell Response in Nerve Regeneration. *Int. J. Mol. Sci.* **2021**, *22*, No. 7901.

(5) Modrak, M.; Talukder, M. A. H.; Gurgenashvili, K.; Noble, M.; Elfar, J. C. Peripheral nerve Injury and Myelination: Potential therapeutic strategies. *J. Neurosci. Res.* **2020**, *98*, 780−795.

(6) Xu, Y.; Zhang, Z.; Chen, X.; Li, R.; Li, D.; Feng, S. A Silk Fibroin/Collagen Nerve Scaffold Seeded with a Co-Culture of Schwann Cells and Adipose-Derived Stem Cells for Sciatic Nerve Regeneration. *PLoS One* **2016**, *11*, No. e0147184.

(7) Kubiak, C. A.; Kung, T. A.; Brown, D. L.; Cederna, P. S.; Kemp, S.W.P. State-of-the-Art Techniques in Treating Peripheral Nerve Injury. *Plast. Reconstr. Surg.* **2018**, *141*, 702−710.

(8) Vijayavenkataraman, S. Nerve Guide Conduits for Peripheral Nerve Injury Repair: A Review on Design, Materials and Fabrication Methods. *Acta Biomater.* **2020**, *106*, 54−69.

(9) Hsiang, S. W.; Tsai, C. C.; Tsai, F. J.; Ho, T. Y.; Yao, C. H.; Chen, Y. S. Novel Use of Biodegradable Casein Conduits for Guided Peripheral Nerve Regeneration. *J. R. Soc., Interface* **2011**, *8*, 1622−1634.

(10) Lupu, M. A.; Gradisteanu Pircalabioru, G.; Chifiriuc, M. C.; Albulescu, R.; Tanase, C. Beneficial Effects of Food Supplements Based on Hydrolyzed Collagen for Skin Care (Review). *Exp. Ther. Med.* **2020**, *20*, 12−17.

(11) Kilmer, C. E.; Battistoni, C. M.; Cox, A.; Breur, G. J.; Panitch, A.; Liu, J. C. Collagen Type I and II Blend Hydrogel with Autologous Mesenchymal Stem Cells as a Scaffold for Articular Cartilage Defect Repair. *ACS Biomater. Sci. Eng.* **2020**, *6*, 3464−3476.

(12) Majumdar, S.; Wang, X.; Sommerfeld, S. D.; Chae, J. J.; Athanasopoulou, E. N.; Shores, L. S.; et al. Cyclodextrin Modulated Type I Collagen Self-Assembly to Engineer Biomimetic Cornea Implants. *Adv. Funct. Mater.* **2018**, *28*, No. 1804076.

(13) Whitlock, E. L.; Tuffaha, S. H.; Luciano, J. P.; Yan, Y.; Hunter, D. A.; Magill, C. K.; et al. Processed Allografts and Type I Collagen Conduits for Repair of Peripheral Nerve Gaps. *Muscle Nerve* **2009**, *39*, 787−799.

(14) Jiang, Y. H.; Lou, Y. Y.; Li, T. H.; Liu, B. Z.; Chen, K.; Zhang, D. Cross-linking Methods of Type I Collagen-based Scaffolds for Cartilage Tissue Engineering. *Am. J. Transl. Res.* **2022**, *14*, 1146−1159.

(15) Qin, L.; Gao, H.; Xiong, S.; Jia, Y.; Ren, L. Preparation of Collagen/Cellulose Nanocrystals Composite Films and Their Potential Applications in Corneal Repair. *J. Mater. Sci. Mater. Med.* **2020**, *31*, No. 55.

(16) Granata, G.; Stracquadanio, S.; Leonardi, M.; Napoli, E.; Malandrino, G.; Cafiso, V.; et al. Oregano and Thyme Essential Oils Encapsulated in Chitosan Nanoparticles as Effective Antimicrobial Agents against Foodborne Pathogens. *Molecules* **2021**, *26*, No. 4055.
(17) Zhang, M. X.; Zhao, W. Y.; Fang, Q. Q.; Wang, X. F.; Chen, C. Y.; Shi, B. H.; et al. Effects of Chitosan-collagen Dressing on Wound Healing in Vitro and in Vivo Assays. *J. Appl. Biomater. Funct. Mater.* **2021**, *19*, No. 2280800021989698.
(18) Korpayev, S.; Kaygusuz, G.; Sen, M.; Orhan, K.; Oto, C.; Karakecili, A. Chitosan/collagen Based Biomimetic Osteochondral Tissue Constructs: A Growth Factor-free Approach. *Int. J. Biol. Macromol.* **2020**, *156*, 681−690.
(19) Everts, P.; Onishi, K.; Jayaram, P.; Lana, J. F.; Mautner, K. Platelet-Rich Plasma: New Performance Understandings and Therapeutic Considerations in 2020. *Int. J. Mol. Sci.* **2020**, *21*, No. 7794.
(20) Yu, W.; Wang, J.; Yin, J. Platelet-rich Plasma: A Promising Product for Treatment of Peripheral Nerve Regeneration After Nerve Injury. *Int. J. Neurosci.* **2011**, *121*, 176−180.
(21) Bastami, F.; Vares, P.; Khojasteh, A. Healing Effects of Platelet-Rich Plasma on Peripheral Nerve Injuries. *J. Craniofacial Surg.* **2017**, *28*, e49−e57.
(22) de Castro, M. V.; da Silva, M. V. R.; Chiarotto, G. B.; Volpe, B. B.; Santana, M. H.; Luzo, Â. C. M.; de Oliveira, A. L. R. Reflex Arc Recovery After Spinal Cord Dorsal Root Repair with Platelet Rich Plasma (PRP). *Brain Res. Bull.* **2019**, *152*, 212−224.
(23) Carvalho, C. R.; Reis, R. L.; Oliveira, J. M.Fundamentals and Current Strategies for Peripheral Nerve Repair and Regeneration. In *Bioinspired Biomaterials*; Chun, H. J.; Reis, R. L., Eds.; Advances in Experimental Medicine and Biology; Springer: Singapore, 2020; Vol. *1249*, pp 173−201.
(24) Gao, D.; Huang, Y.; Sun, X.; Yang, J.; Chen, J.; He, J. Overexpression of C-Jun Inhibits Erastin-induced Ferroptosis in Schwann Cells and Promotes Repair of Facial Nerve Function. *J. Cell. Mol. Med.* **2022**, *26*, 2191−2204.
(25) Zhu, Y.; Jin, Z.; Fang, J.; Wang, J.; Wang, Y.; Song, Q.; et al. Platelet-Rich Plasma Combined with Low-Dose Ultrashort Wave Therapy Accelerates Peripheral Nerve Regeneration. *Tissue Eng., Part A* **2020**, *26*, 178−192.
(26) Reza, M. M.; Subramaniyam, N.; Sim, C. M.; Ge, X.; Sathiakumar, D.; McFarlane, C.; et al. Irisin is a Pro-myogenic Factor That Induces Skeletal Muscle Hypertrophy and Rescues Denervation-induced Atrophy. *Nat. Commun.* **2017**, *8*, No. 1104.
(27) Samadian, H.; Ehterami, A.; Sarrafzadeh, A.; Khastar, H.; Nikbakht, M.; Rezaei, A.; Chegini, L.; Salehi, M. Sophisticated polycaprolactone/gelatin nanofibrous nerve guided conduit containing platelet-rich plasma and citicoline for peripheral nerve regeneration: In vitro and in vivo study. *Int. J. Biol. Macromol.* **2020**, *150*, 380−388.
(28) Singh, P.; Kongara, K.; Harding, D.; Ward, N.; Dukkipati, V.S.R.; Johnson, C.; Chambers, P. Comparison of Electroencephalographic Changes in Response to Acute Electrical and Thermal Stimuli with the Tail Flick and Hot Plate Test in Rats Administered with Opiorphin. *BMC Neurol.* **2018**, *18*, No. 43.
(29) Nakhaee, S.; Dastjerdi, M.; Roumi, H.; Mehrpour, O.; Farrokhfall, K. N-acetylcysteine Dose-dependently Improves the Analgesic Effect of Acetaminophen on the Rat Hot Plate Test. *BMC Pharmacol. Toxicol.* **2021**, *22*, No. 4.
(30) Salehi, M.; Naseri-Nosar, M.; Ebrahimi-Barough, S.; Nourani, M.; Vaez, A.; Farzamfar, S.; Ai, J. Regeneration of Sciatic Nerve Crush Injury by a Hydroxyapatite Nanoparticle-containing Collagen Type I Hydrogel. *J. Physiol. Sci.* **2018**, *68*, 579−587.
(31) Shang, X.; Wang, L.; Liu, Y.; Liu, X.; Lv, J.; Zhou, X.; et al. Diagnostic Value of CXCR3 and its Ligands in Spinal Tuberculosis. *Exp. Ther. Med.* **2020**, *21*, No. 73.
(32) Zhou, J.; Li, S.; Gao, J.; Hu, Y.; Chen, S.; Luo, X.; et al. Epothilone B Facilitates Peripheral Nerve Regeneration by Promoting Autophagy and Migration in Schwann Cells. *Front. Cell. Neurosci.* **2020**, *14*, No. 143.
(33) Gordon, T.; Hendry, M.; Lafontaine, C. A.; Cartar, H.; Zhang, J. J.; Borschel, G. H. Nerve Cross-bridging to Enhance Nerve Regeneration in a Rat Model of Delayed Nerve Repair. *PLoS One* **2015**, *10*, No. e0127397.
(34) Sahana, T. G.; Rekha, P. D. Biopolymers: Applications in Wound Healing and Skin Tissue Engineering. *Mol. Biol. Rep.* **2018**, *45*, 2857−2867.
(35) Real, D. A.; Martinez, M. V.; Frattini, A.; Soazo, M.; Luque, A. G.; Biasoli, M. S.; et al. Design, Characterization, and in Vitro Evaluation of Antifungal Polymeric Films. *AAPS PharmSciTech* **2013**, *14*, 64−73.
(36) Wang, J.; Xiong, H.; Zhu, T.; Liu, Y.; Pan, H.; Fan, C.; et al. Bioinspired Multichannel Nerve Guidance Conduit Based on Shape Memory Nanofibers for Potential Application in Peripheral Nerve Repair. *ACS Nano* **2020**, *14*, 12579−12595.
(37) Kisling, A.; Lust, R. M.; Katwa, L. C. What is the Role of Peptide Fragments of Collagen I and IV in Health and Disease? *Life Sci.* **2019**, *228*, 30−34.
(38) Samadian, H.; Vaez, A.; Ehterami, A.; Salehi, M.; Farzamfar, S.; Sahrapeyma, H.; Norouzi, P. Sciatic Nerve Regeneration by Using Collagen Type I Hydrogel Containing Naringin. *J. Mater. Sci.: Mater. Med.* **2019**, *30*, No. 107.
(39) Marques, C. F.; Diogo, G. S.; Pina, S.; Oliveira, J. M.; Silva, T. H.; Reis, R. L. Collagen-based Bioinks for Hard Tissue Engineering Applications: a Comprehensive Review. *J. Mater. Sci.: Mater. Med.* **2019**, *30*, No. 32.
(40) Tang, R. F.; Zhou, X. Z.; Niu, L.; Qi, Y. Y. Type I Collagen Scaffold with WNT5A Plasmid for in Situ Cartilage Tissue Engineering. *Biomed. Mater. Eng.* **2022**, *33*, 65−76.
(41) Kong, Y.; Wang, D.; Wei, Q.; Yang, Y. Nerve Decellularized Matrix Composite Scaffold With High Antibacterial Activity for Nerve Regeneration. *Front. Bioeng. Biotechnol.* **2022**, *9*, No. 840421.
(42) Boni, R.; Ali, A.; Shavandi, A.; Clarkson, A. N. Current and Novel Polymeric Biomaterials for Neural Tissue Engineering. *J. Biomed. Sci.* **2018**, *25*, No. 90.
(43) Schuh, C. M.; Day, A.G.E.; Redl, H.; Phillips, J. An Optimized Collagen-Fibrin Blend Engineered Neural Tissue Promotes Peripheral Nerve Repair. *Tissue Eng., Part A* **2018**, *24*, 1332−1340.
(44) Chu, C.; Deng, J.; Cao, C.; Man, Y.; Qu, Y. Evaluation of Epigallocatechin-3-gallate Modified Collagen Membrane and Concerns on Schwann Cells. *Biomed. Res. Int.* **2017**, *2017*, No. 9641801.
(45) Ding, T.; Lu, W. W.; Zheng, Y.; Li, Z.; Pan, H.; Luo, Z. Rapid Repair of Rat Sciatic Nerve Injury using a Nanosilver-embedded Collagen Scaffold Coated with Laminin and Fibronectin. *Regener. Med.* **2011**, *6*, 437−447.
(46) Otahal, A.; Kramer, K.; Kuten-Pella, O.; Moser, L. B.; Neubauer, M.; Lacza, Z.; et al. Effects of Extracellular Vesicles from Blood-Derived Products on Osteoarthritic Chondrocytes within an Inflammation Model. *Int. J. Mol. Sci.* **2021**, *22*, No. 7224.
(47) Trull-Ahuir, C.; Sala, D.; Chismol-Abad, J.; Vila-Caballer, M.; Lison, J. F. Efficacy of Platelet-rich Plasma as an Adjuvant to Surgical Carpal Ligament Release: a Prospective, Randomized Controlled Clinical Trial. *Sci. Rep.* **2020**, *10*, No. 2085.
(48) Censi, R.; Casadidio, C.; Deng, S.; Gigliobianco, M. R.; Sabbieti, M. G.; Agas, D.; et al. Interpenetrating Hydrogel Networks Enhance Mechanical Stability, Rheological Properties, Release Behavior and Adhesiveness of Platelet-Rich Plasma. *Int. J. Mol. Sci.* **2020**, *21*, No. 1339.
(49) Park, K.; Shin, Y.; Lee, G.; Park, H.; Choi, Y. Dabrafenib Promotes Schwann Cell Differentiation by Inhibition of the MEK-ERK Pathway. *Molecules* **2021**, *26*, No. 2141.
(50) Deng, X.; Liang, Y.; Lu, H.; Yang, Z.; Liu, R. E.; Wang, J.; et al. Co-transplantation of GDNF-overexpressing Neural Stem Cells and Fetal Dopaminergic Neurons Mitigates Motor Symptoms in a Rat Model of Parkinson's Disease. *PLoS One.* **2013**, *8*, No. e80880.
(51) Günther, H. S.; Henne, S.; Oehlmann, J.; Urban, J.; Pleizier, D.; Renevier, N.; et al. GFAP and Desmin Expression in Lymphatic Tissues Leads to Difficulties in Distinguishing between Glial and Stromal Cells. *Sci. Rep.* **2021**, *11*, No. 13322.
(52) Cheng, C.; Zochodne, D. W. In Vivo Proliferation, Migration and Phenotypic Changes of Schwann Cells in the Presence of Myelinated Fibers. *Neuroscience* **2002**, *115*, 321−329.

https://doi.org/10.1021/acsomega.2c05351
ACS Omega 2023, 8, 2931−2941